A model for self-sustained potential oscillation of lipid bilayer membranes induced by the gel–liquid crystal phase transitions

Kouichi Yagisawa,* Masayoshi Naito,‡ Ken-Ichiro Gondaira,* and Takeshi Kambara*

*Department of Applied Physics and Chemistry, The University of Electro-Communications, Chofu, Tokyo 182; and ‡Advanced Research Laboratory, Hitachi, Ltd., Hatoyama, Saitama 350-03, Japan

ABSTRACT To clarify the mechanism of self-sustained oscillation of the electric potential between the two solutions divided by a lipid bilayer membrane, a microscopic model of the membrane system is presented. It is assumed, on the basis of the observed results (Yoshikawa, K., T. Omachi, T. Ishii, Y. Kuroda, and K. Iiyama. 1985. *Biochem. Biophys. Res. Commun.* 133:740–744; Ishii, T., Y. Kuroda, T. Omochi, and K. Yoshikawa. 1986. *Langmuir.* 2:319–321; Toko, K., N. Nagashima, S. Iiyama, K. Yamafuji, and T. Kunitake. *Chem. Lett.* 1986:1375–1378), that the gel–liquid crystal phase transition of the membrane drives the potential oscillation. It is studied, by using the model, how and under what condition the repetitive phase transition may occur and induce the potential oscillation. The transitions are driven by the repetitive adsorption and desorption of proton by the membrane surface, actions that are induced by the periodic reversal of the direction of protonic current. The essential conditions for the periodic reversal are (*a*) at least one kind of cations such as Na^+ or K^+ are included in the system except for proton, and the variation of their permeability across the membrane due to the phase transition is noticeably larger than that of proton permeability; and (*b*) the phase transition has a hysteresis. When these conditions are fulfilled, the self-sustained potential oscillation may be brought about by adjusting temperature, pH, and the cation concentration in the solutions on both sides of the membrane. Application of electric current across the membrane also induces or modifies the potential oscillation. Periodic, quasiperiodic, and chaotic oscillations appear especially, depending on the value of frequency of the applied alternating current.

INTRODUCTION

Characteristic variations of cellular membrane potential play a quite important role in many kinds of cellular function, such as transduction of stimuli, signaling, regulation, movement, and development. Although the mechanism of the potential variation has been actively investigated through various approaches, our understanding of the mechanism at the molecular level is not yet systematic enough. It has been suggested by many workers (1–6) that the molecular mechanism is essentially based on conformation changes in the membranes. The main constituents of the membranes responsible for the potential changes are the proteins, such as the ion channels and receptors, and the lipid bilayers. Numerous workers have postulated (for example, reference 7) that a conformation change of the relevant proteins occurs during the membrane excitation. The membrane fluidity arising from the dynamics of lipid molecules significantly affects the cation permeability across the membrane (8) and the transmembrane potential (5, 9, 10). These observed results suggest the importance of the contribution of the lipid bilayer to the membrane conformation change associating with the potential variation. However, the role of lipid bilayers is not yet clear compared with that of the proteins.

In this paper we are concerned about the role of lipid bilayers in the conformation change of membranes responsible for the characteristic potential variations. To make our problem clear, we choose the gel-liquid crystal phase transition as a typical conformation change and consider the self-sustained oscillation as a characteristic potential variation. The gel-liquid crystalline phase transition of lipid bilayers is one of the most plausible conformation changes, although so far no direct evidence supports the idea that the phase transitions are actively involved in biological processes. Numerous studies (for example, reference 11) have demonstrated that many organisms adjust the lipid composition of their membranes so that a small fraction of their membranes are in the gel phase at the growth temperature. Vaz et al. (12) indicated that the coexistence of gel and liquid crystalline phases in the membrane was used to realize some functions of the membranes. Träuble and Eibl (13) showed that the phase transition could be triggered by a variation in the molar ratio of mono- and divalent cation. They suggested, on the basis of the observed results, that the phase transitions were actively involved in the axonal membrane excitation. Blatt (14) also suggested, on the basis of the observation of temperature dependence of the action potential in the *Nitella flexilis,* that a drastic change of the action potential with temperature arose from the lipid phase transition. DeSimone and Heck (15) suggested that the taste transduction was triggered by the phase transition of receptor membrane induced by chemical stimuli.

The more direct observations have been reported about the relation between the potential variation and phase transition in lipid bilayer membranes. Antonov et al. (16) showed that the pulse-like fluctuation of ionic current across the membranes appeared under applied voltage at the phase transition temperature of lipid bilayers. Toko et al. (17) found that the self-sustained potential oscillation in the synthetic multi-bilayer mem-

Address correspondence to T. Kambara.

0006-3495/93/05/1461/15 $2.00

branes occurred under the salt concentration gradient and that the oscillation was associated with the gel-liquid crystal phase transition of the membranes. Yoshikawa et al. (18) and Ishii et al. (19) showed that spontaneous potential oscillation occurred across a Langmuir–Blodgett film of dioleyllecithin when it was imposed between aqueous solutions of equimolar NaCl and KCl. They suggested that the potential oscillations were due to the repetitive phase transitions between the two membrane states with high and low resistances.

To obtain a better understanding of the mechanism by which the gel-liquid crystal phase transitions may induce the self-sustained oscillation of the membrane potential, we present a microscopic model of the system where two kinds of aqueous solutions are divided by a lipid bilayer membrane and investigate by the use of the model how the phase transition couples with the potential changes induced by the external chemical and electrical stimulations. The driving force of the phase transition is the repetitive adsorption and desorption of proton by the polar heads of acidic lipid molecules. The adsorption stabilizes the gel state and the desorption stabilizes the liquid crystal state. The membrane potential arising from the ion diffusion across the membrane is changed markedly with the phase transition, because the ion permeability is quite different between the gel and liquid crystal states. The repetition of proton adsorption and desorption is induced by the periodic reversal of the direction of protonic current in the membrane. The periodic reversal is brought about by the specific type of the phase transition of the bilayer membrane, in that the repetitive phase transition occurs only in one half of the bilayer and the other half stays in the gel state or the liquid crystal state.

The wave form of the potential oscillation is varied by changing the ionic concentrations in the solution region far from the membrane, temperature, or the applied electric current. Periodic, quasiperiodic, and chaotic oscillations appear especially, depending on the value of frequency of the applied alternating current.

THEORETICAL MODEL

Model for the lipid membrane system

We consider a model system in which a lipid bilayer membrane is in aqueous solution and divides the solution into two regions. The bilayers considered consist of neutral and acidic lipid molecules, where the acidic molecule has a net negative charge in the ionized state. The ion species considered in the aqueous solution regions are proton H^+, hydroxide OH^-, one kind of alkaline ion M^+, and one kind of halogen ion A^-.

There exist three kinds of regions with respect to the ion distribution in the present system, as shown in Fig. 1: they are the bilayer membrane ($-l < x < l$), the bulk solutions ($-L < x < -\lambda$ and $\lambda < x < L$), and the diffuse

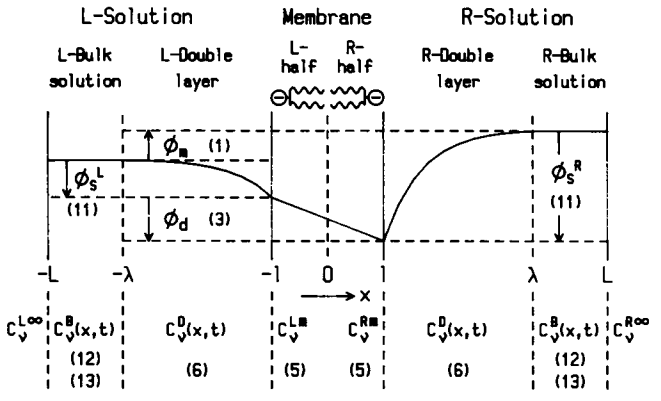

FIGURE 1 Cross-sectional drawing of the present system of a lipid bilayer membrane dividing the solution into the two regions. Each solution consists of the bulk solution and the double-layer region. The electric potential ϕ and ion concentration C_ν are shown for each region. The numbers attached to ϕ and C_ν denote the relevant equations in the text.

electric double-layer regions ($-\lambda < x < -l$ and $l < x < \lambda$) produced by the membrane surface charges. The potential gradient is produced in the double-layer regions by the surface charges, as shown in Fig. 1. Because the effect of surface charges is screened by the double layer, the bulk solution regions are electrically neutral and the electric potential is almost constant there. The ions diffused in the bulk solution reach the membrane surface through the double layer and permeate into the lipid membrane region at the rate of the partition coefficient between the aqueous solution and the lipid membrane.

We assume that the distribution of the negative charges on the membrane surfaces arising from the ionized lipid molecules is smoothed throughout the surfaces, because the lateral exchange period of the molecules ($\sim 10^{-7}$ s) is much shorter than the potential oscillation period ($\geq 10^{-3}$ s) (20). Then, the ion distributions and, as a result, the potentials are uniform in a plane parallel to the membrane. We hereafter consider the spatial variation of the physical quantities only along the direction perpendicular to the membrane.

The membrane potential is defined as the potential difference between the two bulk solutions across the membrane. Then, the membrane potential ϕ_m is obtained by

$$\phi_m = \phi_s^L + \phi_d - \phi_s^R, \qquad (1)$$

as shown in Fig. 1. Here, ϕ_s^L and ϕ_s^R are the surface potentials at the left and right solution regions, respectively, and are produced by the membrane surface charges. The ion permeation through the membrane induces the transmembrane potential difference ϕ_d, and hereafter we call it the diffusion potential.

When the difference in the ion concentration between the left and right bulk solutions is maintained, the ions flow continuously across the membrane. Because the cat-

ions are adsorbed on the ionized polar heads of acidic lipid, the cation flow modifies the surface charge density of the membrane. The modification may induce the gel-liquid crystal phase transition of lipid membrane, because the liquid crystal state is more stabilized with increasing of the negative surface charge. The diffusion potential ϕ_d is changed drastically by the phase transition, because the ion partition coefficients for the membrane in the gel state are quite different from those for the membrane in the liquid crystal state. If the direction of cation flow is reversed repetitively, the oscillation of membrane potential ϕ_m is the result in the present system. The condition under which the repetitive reversal of cation flow may occur is described in the next section. In the following two subsections, we present the basic equations required for the membrane potential and describe the gel-liquid crystal phase transition, to explain the problem mathematically.

Basic equations for the membrane potential

We derive here the basic equations that determine the time dependence of membrane potential ϕ_m. The membrane potential ϕ_m arises from the left and right surface potentials, ϕ_s^L and ϕ_s^R, and the diffusion potential ϕ_d, as shown in Eq. 1 and Fig. 1.

First, we derive the equation for the diffusion potential ϕ_d. The total electric current J flowing through the membrane consists of ionic and displacement currents and is represented as

$$J = F \sum_\nu z_\nu \Phi_\nu^m + \epsilon_m \frac{\partial E_m}{\partial t}, \tag{2}$$

where the suffix ν stands for ion species (ν = H for proton, OH for hydroxide, M for alkaline ion, and A for halogen ion), Φ_ν^m is the flux (mol/m^2 s) of the ion ν across the membrane, z_ν is its valency, ϵ_m is the dielectric constant of the membrane, E_m is the electric field in the membrane, and F is the Faraday constant. Because the electric field is reasonably treated as spatially constant in such thin films as the biological membranes (21), E_m is given by ϕ_d as $E_m = -\phi_d/(2l)$, where $2l$ is the thickness of the membrane. Then, Eq. 2 is rewritten as

$$\frac{d\phi_d}{dt} = \frac{2l}{\epsilon_m} F \sum_\nu z_\nu \Phi_\nu^m - \frac{2l}{\epsilon_m} J. \tag{3}$$

It is clear from continuity of electric current that J is equivalent to the external electric current applied as a stimulation. The ion flux Φ_ν^m is represented by Goldman's expression (22), even for transient states considered here (21), as

$$\Phi_\nu^m = \frac{D_\nu^m}{2l} \frac{z_\nu F}{2RT} \frac{\phi_d}{\sinh(z_\nu F\phi_d/2RT)} \times \left[C_\nu^{Lm} \exp\left(-\frac{z_\nu F\phi_d}{2RT}\right) - C_\nu^{Rm} \exp\left(\frac{z_\nu F\phi_d}{2RT}\right) \right], \tag{4}$$

where C_ν^{Lm} and C_ν^{Rm} are the ν ion concentrations at the left and right ends ($x = -l$ and l) in the membrane, respectively, and D_ν^m is the diffusion constant (m^2/s) of the ion ν in the membrane.

When the values of C_ν^{Xm} (X = L or R) are given as functions of time, the time dependence of ϕ_d is obtained using Eqs. 3 and 4. We represent C_ν^{Xm} using the ionic concentrations in the double layer regions as

$$C_\nu^{Xm} = k_\nu^X C_\nu^D(l_X, t), \quad (X = L, R), \tag{5}$$

where $C_\nu^D(l_X, t)$ is the concentration of ion ν in the X-side double-layer region at the membrane surface ($l_X = -l$ for X = L, $l_X = l$ for X = R), and k_ν^X is the partition coefficient of ion ν between the X-side half of the bilayer and the X-side solution. The values of $D_\nu^m k_\nu^X/2l$ corresponding to the permeability of ion ν depend on the state of the X-side half, as described in the next subsection.

The equations for $C_\nu^D(l_X, t)$ and the surface potentials ϕ_s^L and ϕ_s^R are derived by considering the ion distributions in the double-layer regions. The ion distributions in the regions are close to the thermal equilibrium ones, because the relaxation time ($\lambda^2/D_\nu^S \simeq 10^{-6}$ s) of the ion distribution is much shorter than the period of potential oscillation ($\sim$1 s) and so the relaxation of ion distribution is much faster than the process of ion diffusion in the bulk solution region, which disturbs the ion distribution (23). Therefore, we approximate $C_\nu^D(x, t)$ with the ion concentration in the thermal equilibrium state as

$$C_\nu^D(x, t) \simeq \begin{cases} C_\nu^B(\lambda_X, t)\{\coth \tfrac{1}{2}[\kappa_X(x - l_X) + a_X]\}^2 \\ \quad \text{for} \quad \nu = H, M \\ C_\nu^B(\lambda_X, t)\{\tanh \tfrac{1}{2}[\kappa_X(x - l_X) + a_X]\}^2 \\ \quad \text{for} \quad \nu = OH, A, \end{cases} \tag{6}$$

where λ_X is λ for X = R and $-\lambda$ for X = L, and $C_\nu^B(x, t)$ is the concentration of ion ν in the bulk solution. The quantities κ_X and a_X (X = L, R) are defined by

$$\kappa_X = \left(\frac{F}{2RT\epsilon_s} Q_X\right)^{1/2}, \tag{7}$$

$$a_X = \left(\frac{\lambda_X}{\lambda}\right) \ln\left[\left(1 + \frac{Q_X}{W_X}\right)^{1/2} - \left(\frac{Q_X}{W_X}\right)^{1/2}\right], \tag{8}$$

where

$$Q_X = F \sum_{\nu=H,M} C_\nu^B(\lambda_X, t), \tag{9}$$

$$W_X = \frac{F}{8RT\epsilon_s}\left(\frac{\epsilon_m}{2l}\phi_d - \frac{\lambda_X}{\lambda}\sigma_X\right)^2, \tag{10}$$

where ϵ_s is the dielectric constant of the aqueous solution, and σ_X is the fixed charge at the X-side membrane surface. Eq. 6 is derived from the Poisson equation with the boundary conditions at $x = \lambda_X$ and $x = l_X$, as shown in Appendix A. The surface potentials ϕ_s^X are also obtained by using the potential $\phi(x, t)$ in the double-layer region and represented as

$$\phi_s^X = \phi(l_X, t) - \phi(\lambda_X, t) = -\frac{2RT}{F} \ln\left[\left(1 + \frac{W_X}{Q_X}\right)^{1/2} + \left(\frac{W_X}{Q_X}\right)^{1/2}\right]. \quad (11)$$

To solve Eq. 3 for ϕ_d and Eq. 11 for ϕ_s^X, we need the equations determining $C_\nu^B(\lambda_X, t)$ and σ_X. The ion concentration $C_\nu^B(x, t)$ in the bulk solution is determined by the diffusion equation under the boundary conditions that $C_\nu^B(x, t)$ takes the fixed value $C_\nu^{X\infty}$ at $x = L_X$ and the ion flux $(-D_\nu^S \partial C_\nu^B(x, t)/\partial x)$ takes $\Phi_\nu^{X\lambda}(t)$ at $x = \lambda_X$. The solutions for the alkaline and halogen ions (ν = M and A) are

$$C_\nu^B(x, t) = C_\nu^{X\infty} + \left(\frac{\lambda_X}{\lambda}\right) \int_0^\infty \Phi_\nu^{X\lambda}(t - u) u^{-1/2} \times \exp\left[-\frac{(x - \lambda_X)}{4D_\nu^S u}\right] du, \quad (12)$$

where D_ν^S is the diffusion constant of the ion ν in the bulk solution. The concentrations for H^+ and OH^- are represented under the equilibrium condition of ($H^+ + OH^- \rightleftharpoons H_2O$) as

$$C_H^B(x, t) - C_{OH}^B(x, t) = C_H^{X\infty} - C_{OH}^{X\infty} + \left(\frac{\lambda_X}{\lambda}\right) \times \int_0^\infty [\Phi_H^{X\lambda}(t - u) - \Phi_{OH}^{X\lambda}(t - u)] \times u^{-1/2} \exp\left[-\frac{(x - \lambda_X)}{4D_H^S u}\right] du, \quad (13)$$

$$C_H^B(x, t) C_{OH}^B(x, t) = K_W, \quad (14)$$

where K_W is the ion product of water. The derivation of Eqs. 12 and 13 is explained briefly in Appendix B. The ion flux $\Phi_\nu^{X\lambda}(t)$ across the plane of $x = \lambda_X$ is obtained from the ion conservation equation in the X-side double-layer region,

$$\Phi_\nu^{X\lambda}(t) = \Phi_\nu^m - \left(\frac{\lambda_X}{\lambda}\right) \frac{d}{dt} Q_\nu^X(t), \quad (15)$$

$$Q_\nu^X(t) = C_\nu^B(\lambda_X, t) \times \left\{\lambda - l + \frac{2}{\kappa_X}\left[\left(1 + \frac{W_X}{Q_X}\right)^{1/2} - 1 + z_\nu\left(\frac{W_X}{Q_X}\right)^{1/2}\right]\right\}, \quad (16)$$

where Φ_ν^m is given by Eq. 4, $Q_\nu^X(t)$ is the total amount of ion ν in the X-side double-layer region, and the derivation of $Q_\nu^X(t)$ is shown in Appendix A.

Finally, we give the expression of the fixed surface charge σ_X in terms of the cation concentration $C_\nu^D(x, t)$ at the membrane surface ($x = l_X$). The surface charges arise from the ionized polar heads (P^-) of acidic lipid. Because cations H^+ and M^+ are adsorbed on P^-, we consider the adsorption and desorption processes, $H^+ + P^- \rightleftharpoons HP$ and $M^+ + P^- \rightleftharpoons MP$. It is highly reasonable that the adsorption equilibrium is attained every moment during the potential oscillation, because the adsorption processes are much faster than the rate of potential variation. Assuming the Langmuir isotherm for the adsorption probability, we obtain σ_X (X = R, L) as

$$\sigma_X = \frac{-FA_{LM}\xi_X}{1 + \sum_{\nu=H,M} K_\nu C_\nu^D(l_X, t)}, \quad (17)$$

where A_{LM} is the areal density of lipid molecules in the membrane, ξ_X is the fraction of acidic lipids on the X-side half of the bilayer, and K_ν is the association constant (m^3/mol) in the adsorption of ion ν.

Description of conformation change of the membrane system

To study the effect of conformation change of lipid bilayer to the membrane potential, we choose the gel-liquid crystal phase transition of the bilayer as a typical conformation change. In the phase transition, the hydrocarbon chains of lipid molecules change from an all-*trans*, rigid extended conformation in the gel phase to a highly degenerate rotational isomeric, shortened kink-containing conformation in the liquid crystal phase. The phase transition can be induced by the proton adsorption on the polar heads of acidic lipid, because the proton adsorption reduces the coulomb repulsion between the acidic lipid molecules and stabilizes the gel state, while the proton desorption stabilizes the liquid crystal state (13, 24, 25).

We describe the ion-induced phase transition based on the two-state model (26–28), although various theoretical models have been presented for the description of the phase transition induced by the temperature variation (27, 29, 30). We adopt this approach as a minimal model description, which may reproduce the essential parts of macroscopic features in the transition phenomena. There are some features of the membranes near the gel-liquid crystal phase transitions, such as lateral density fluctuations, that may not be well described by the minimal model. The effects of the features on the potential oscillations are discussed later. We assume, on the basis of the observed lacking of transbilayer coupling (31), that the two lipid monolayers constituting a bilayer membrane undergo the phase transition independently. The assumption was adopted in most of the previous models, and the models well reproduced the essential features of the transition (27, 29).

Each hydrocarbon chain of lipid molecules in the monolayer can exist in one of the two states, which are the all-*trans* or ground state G and the kink-containing or excited state E. The Gibbs free energy of the lipid monolayer is given by (26)

$$F = N \sum_\alpha [(E_\alpha - TS_\alpha + PA_\alpha)\rho_\alpha + k_B T \rho_\alpha \ln \rho_\alpha] - 3N \sum_{\alpha,\beta} J_{\alpha\beta}\rho_\alpha\rho_\beta + W_{el}, \quad (18)$$

where N is the total number of hydrocarbon chains; α and β run over G and E; ρ_α is the population ratio of α state; E_α, S_α, and A_α are the intrachain energy and entropy, and chain cross section, respectively, in the α state; P is the effective lateral pressure; $J_{\alpha\beta}$ is the interaction strength between the nearest neighboring chains in the α and β states; and W_{el} is the coulomb interaction between the ionized lipid molecules. The coulomb interaction W_{el} is represented as

$$W_{el} = Nw\left(\rho_G + \frac{A_E}{A_G}\rho_E\right)^{-1/2}, \quad (19)$$

where the derivation of Eq. 19 and the meaning of w are given in Appendix C.

The gel-liquid crystal phase transition is described by the order parameter η, which is defined as

$$\eta = \rho_G - \rho_E = 1 - 2\rho_E. \quad (20)$$

The gel and liquid crystal states correspond to $\eta = 1$ and -1, respectively. The value of η is determined by

$$\tau_{PT}\frac{d\eta}{dt} = -\frac{1}{N}\frac{\partial F}{\partial \eta} = -\frac{1}{2}k_BT\ln\left(\frac{1+\eta}{1-\eta}\right) + g_0 + g_1\eta + \frac{1}{\sqrt{2}}w\left[1 - \frac{A_E}{A_G} + \left(1 - \frac{A_E}{A_G}\right)\eta\right]^{-3/2}, \quad (21)$$

$$g_0 = \tfrac{1}{2}[E_E - E_G - T(S_E - S_G) + P(A_E - A_G) + 3(J_{GG} - J_{EE})], \quad (22)$$

$$g_1 = \tfrac{3}{2}(J_{GG} + J_{EE} - 2J_{GE}). \quad (23)$$

Because the time constant τ_{PT} of the gel-liquid crystal phase transition is extremely short compared with the period of potential oscillation, as shown in the next section, we can safely treat the membrane conformation as the stationary state, that is, $d\eta/dt = 0$. Then, η corresponds to the thermal equilibrium state determined so as to minimize the free energy F.

The equation $\partial F/\partial\eta = 0$ has various kinds of solutions η depending on the value of the electric interaction strength w. The proton flux across the membrane changes the value of w, because w depends on the membrane surface charge, as shown in Appendix C. We describe briefly how the phase transition is induced through the variation of w. When w is within the region of $(w_0 - \Delta w < w < w_0 + \Delta w)$, the equation $\partial F/\partial\eta = 0$ has simultaneously three solutions (η_l, η_u, η_g), where $2\Delta w$ is the width of the critical region of w; η_l and η_g correspond to the liquid crystal and gel states, respectively; and η_u corresponds to the unstable state. The liquid crystal state is more stable, that is, $F(\eta_l) < F(\eta_g)$, for $w > w_0$; the gel state is more stable for $w < w_0$; and the two states may coexist for $w = w_0$, that is, $F(\eta_l) = F(\eta_g)$. It has been shown experimentally that the phase transition induced by cation adsorption has a hysteresis, as does the thermally induced transition (13, 24, 25, 32). Therefore, the value of w at which the phase transition occurs is shifted from w_0. We assume that when w decreases and reaches $w_0 - \gamma\Delta w$ $(0 < \gamma < 1)$, the state (η) of the lipid monolayer changes abruptly from the liquid crystal state (η_l) to the gel state (η_g), and when w increases and reaches $w_0 + \gamma\Delta w$, the state changes from the gel state (η_g) to the liquid crystal one (η_l). This hysteresis is one of the essential mechanisms inducing the self-sustained potential oscillations in the present model.

It is well known (27, 33–35) that the ion permeability across lipid mono- and bilayers changes drastically with the gel-liquid crystal phase transition. We approximate the potential barrier height by a quadratic equation of the order parameter η. Then, the permeability $D_\nu^m k_\nu^X/(2l)$ for the ν ion across the X-side monolayer (X = R, L) is represented as

$$D_\nu^m k_\nu^X/(2l) = P_\nu^X \exp\left[-\frac{\epsilon_{\nu 1}^X \eta_X - \epsilon_{\nu 2}^X(1 - \eta_X^2)}{k_BT}\right], \quad (24)$$

where P_ν^X is the constant term, $\epsilon_{\nu 1}^X$ is the term representing the difference between the gel $(\eta_X = 1)$ and the liquid crystal $(\eta_X = -1)$ states, and $\epsilon_{\nu 2}^X$ is the term arising from the density fluctuation around the transition point $(\eta_X \simeq 0)$ (36).

Preparation for numerical calculations

We adopt the values of the quantities included in the present model as shown in Table 1. The values in parentheses and those with underlines mean the standard values, which we use without any statement in the following calculations.

The values of ion permeabilities have been obtained for various lipid liposomes. The values, however, scatter in the range from 10^{-12} to 10^{-16} m/s for monovalent cations such as Na^+, K^+, or Rb^+ (37–42), and also from 10^{-5} to 10^{-9} m/s for H^+/OH^- (40, 43–48). The permeability of Cl^- has been estimated to be 10–100 times the value for alkaline ions (38, 39). It has been observed for proton (25) that the ratio of partition coefficient in the gel state to that in the liquid crystal state is ~1:10. We take the values of P_ν^X and ϵ_{H1}^X, as shown in Table 1, on the basis of the observed results. We assume for simplicity that $\epsilon_{OH1}^X = \epsilon_{A1}^X = \epsilon_{H1}^X$, because the contribution of anion to the potential oscillation is small. We assume also that the change of partition coefficient due to the phase transition is larger for the cation M^+ than for H^+, because the hydrated ion size of M^+ is much larger than that of H^+. Then, we take a value in the range of 500–1,500k_B as ϵ_{M1}^X. We estimate the values of ϵ_{H2}^X and ϵ_{M2}^X based on the relevant values obtained by Georgallas et al. (36). We assume for simplicity that $\epsilon_{OH2}^X = \epsilon_{A2}^X = \epsilon_{H2}^X$. The value of the association constant K_H of H^+ has been reported to be $10^{4.75}$ M^{-1} for PS (phosphatidylserine) (49), $10^{3.6}$ M^{-1} for the carboxyl group of PS, and $10^{9.8}$ M^{-1} for the amino group of PS (50). We take a value in the range of $10^{3.0}$–$10^{6.0}$ M^{-1} for K_H. Because the association constant K_M of monovalent cation such as Na^+ and

TABLE 1 **Values of the physical quantities included in the present model**

Quantities	Definition	Value
$2l$	Thickness of the bilayer	5 nm
A_G	The cross-section of lipid chain in the ground and excited conformations	0.204 $(nm)^2$
A_E		0.34 $(nm)^2$
ξ_R	The fraction of acidic lipids in the right and left halves of the bilayer	0.3–0.8 (0.3)
ξ_L		0.3–1.0 (0.7)
ϵ_m	Dielectric constant of the membrane and of the solution	$2\epsilon_0$
ϵ_s		$78\epsilon_0$
P_H^X	Quantities corresponding to permeability of ions H^+, M^+, OH^-, and A^-	10^{-9}–10^{-5} m/s (5×10^{-7})
P_M^X		10^{-16}–10^{-12} m/s (5×10^{-13})
P_{OH}^X, P_A^X		$P_{OH}^X = P_H^X$, $P_A^X = 10P_M^X$
$\epsilon_{\nu 1}^X$	Parameters relevant to the change of partition coefficient due to the phase transition (Eq. 24)	$\epsilon_{\nu 1}^X = 300k_B$, $\epsilon_{\nu 2}^X = 200k_B$ for ν = H, OH, A
$\epsilon_{\nu 2}^X$		ϵ_{M1}^X = 500–1,500k_B (1,000)
		$\epsilon_{M2}^X = 400k_B$
K_H	Association constant of H^+ and M^+ with the ionized lipid	10^3–10^6 M^{-1} ($10^{4.75}$)
K_M		0
N_C	Number of C—C bonds in the hydrocarbon chain	16, 18, 20
$E_E - E_G$	Differences in energy and entropy of the chain between the excited and ground states (they depend on N_C)	1,794k_B, 2,595k_B, 3,600k_B
$S_E - S_G$		12.78k_B, 14.98k_B, 17.17k_B
J_{GG}	Interaction strengths between the molecules in G and G states, in G and E states, and E and E states	648k_B, 677k_B, 700k_B
J_{GE}		$J_{GE} = 0.148J_{GG}$
J_{EE}		$J_{EE} = 0.022J_{GG}$
P	Lateral pressure in the lipid membrane	33 dyn/cm^2
ω	Parameter relevant to the intermolecular coulomb interaction	5×10^2–$5 \times 10^3 k_B$ (1.7×10^3)
γ	Parameter representing the hysteresis	10^{-3}–10^{-1} (10^{-2})
T	Temperature	200–400 K (323)
$C_H^{R\infty}$	Fixed ionic concentrations in the outside of right and left bulk solution regions	10^{-5}–10^{-3} mol/m^3 ($10^{-4.5}$)
$C_M^{R\infty}$		1–20 mol/m^3 (5)
$C_H^{L\infty}$		10^{-4}–10^{-2} mol/m^3 (10^{-3})
$C_M^{L\infty}$		10–10^2 mol/m^3 (50)
$C_{OH}^{X\infty}$		$C_{OH}^{X\infty} = K_W/C_H^{X\infty}$
$C_A^{X\infty}$		$C_A^{X\infty} = C_H^{X\infty} + C_M^{X\infty} - C_{OH}^{X\infty}$
J	External direct electric current	-1×10^{-3}–1×10^{-3} A/m^2 (0)
$J_0 \sin 2\pi ft$	External alternating current	J_0 = 0.1–1 mA/m^2 (0)
		f = 0.1–10 s^{-1}

The values in parenthesis and those with underlines indicate the standard values mentioned in the text.

K^+ is <1 M^{-1} (51), we neglect the adsorption of M^+ on the ionized lipid molecules.

The values of parameters relevant to the conformation change depend on the number N_C of C—C bonds in the hydrocarbon chain, except for the lateral pressure P and the strength of intermolecular coulomb interaction w, where we adopt Nagle's (29) estimation for P and the estimation of w is shown in Appendix C. For $E_E - E_G$, $S_E - S_G$, J_{GG}, J_{GE}, and J_{EE}, we adopt the relevant estimation of Georgallas et al. (36). The value of the parameter γ representing the hysteresis is taken in the range of 10^{-3}–10^{-1}, because the potential oscillation does not occur in case of the standard values if γ is not within the range.

The externally controllable parameters in the present model are temperature T, the ion concentrations $C_H^{X\infty}$ and $C_M^{X\infty}$ in the outside solution regions (X = R, L), and the electric current J. The anion concentrations $C_{OH}^{X\infty}$ and $C_A^{X\infty}$ are determined by the equations $C_{OH}^{X\infty}C_H^{X\infty} = K_W$ and $C_H^{X\infty} + C_M^{X\infty} - C_A^{X\infty} - C_{OH}^{X\infty} = 0$, where K_W is the ion product of water and 10^{-8} $(mol/m^3)^2$. We use the standard values shown in Table 1 for the external parameters. To investigate the effect of the external condition, we change the value of T, $C_H^{X\infty}$, and $C_M^{X\infty}$ in the neighborhood of the standard values. We apply alternating current as well as direct current to the system. The alternating current is given in the form of $J_0 \sin(2\pi ft)$.

Finally, we consider the value of the relaxation time τ_{PT} for the gel-liquid crystal phase transition as it appears in Eq. 21. Because the value has not been reported, we estimate it as the order of the time scales for the ultrasonic relaxation ($\gtrsim 1$ μs) (52) and for the viscoelastic relaxation (~ 20 μs) (53) in the gel-liquid crystal phase transition of lipid bilayer membranes. Then τ_{PT} is much shorter than the period ($\gtrsim 1$ ms) of the potential oscillation.

CALCULATED RESULTS

Mechanism of self-sustained oscillation

The self-sustained oscillation of the membrane potential ϕ_m is calculated for various values of the parameters and

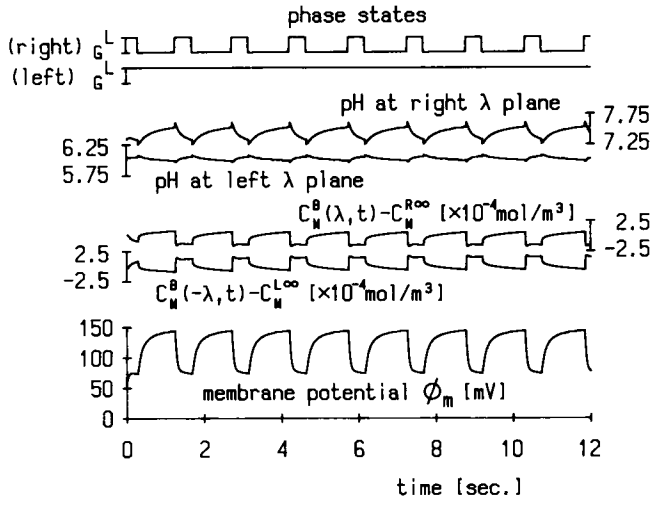

FIGURE 2 The calculated time dependences of the membrane potential ϕ_m and the states of the right and left halves of the bilayer membrane, where L and G mean the liquid crystal and gel states, respectively. The variation of concentrations of proton H^+ and alkaline ion M^+ at both the λ planes ($x = -\lambda, \lambda$) are also shown. The values of parameters used are the standard values given in Table 1.

is shown in Fig. 2 for the standard values of the parameters given in Table 1. Variation patterns of the state of right and left halves of the lipid bilayer are shown in Fig. 2, with the oscillations of concentrations of H^+ and M^+ at both the right and left λ planes shown in Fig. 1.

The self-sustained oscillation of ϕ_m is induced by the repetitive phase transition of lipid membrane, which is driven by the concentration gradients of H^+ and M^+ across the membrane. We explain briefly how and under what condition this process occurs. There are two types of the repetitive phase transitions: (*a*) one half of the bilayer repeats the phase transition between the gel and the liquid crystal states, but the other half remains in the liquid crystal state; (*b*) one half repeates the phase transition, but the other remains in the gel state. We show schematically one cycle of the first type of repetitive phase transition induced by a cyclic change of the direction of H^+ flux in Fig. 3. The gel state of lipid layers is generally stabilized with the H^+ adsorption on ionized polar heads of lipid molecules because of the reduction of coulomb repulsion between charged lipid molecules, while the desorption of H^+ stabilizes the liquid crystal state. Therefore, the state of each half of the bilayer depends on the concentration of H^+ near the surface layer. Because the variation of the H^+ concentration is induced by the H^+ flux across the membrane, the change in the direction of H^+ flux leads the phase transition, as shown in Fig. 3: when H^+ flows enough into the right half being in the liquid crystal state, the state is changed to the gel one. When the permeability of M^+ in the right half decreases more (largely due to the phase transition) than does that of H^+, as in the standard case, the direction of M^+ flux is reversed, because the M^+ flow from the right solution into the right half of the bilayer decreases drastically. Then, the direction of the H^+ flux also is reversed because of the charge neutrality condition, and the H^+ ions adsorbed on the surface of right half begin desorbing. After enough H^+ is desorbed, the state of the half returns to the initial liquid crystal state. Because there exists a hysteresis in the phase transition of lipid layers, the surface concentration of H^+ at which the transition from the gel state to the liquid crystal state occurs is less by a definite amount than the concentration relevant to the reverse transition. This makes the time interval between the successive phase transitions finite.

We consider a little more quantitatively the condition under which the H^+ flux Φ_H^m across membrane changes its direction. Because the fluxes of anions in the membrane are quite small because of the negatively charged surface of the membrane, the total flux of cations, $\Phi_H^m + \Phi_M^m$, in the membrane is near zero. By using Eq. 4 and $\Phi_M^m = -\Phi_H^m$, the sign of Φ_H^m is obtained as

$$\text{sign}\,(\Phi_H^m) = \text{sign}\,(Y_{MR}Y_{HL} - Y_{ML}Y_{HR}), \qquad (25)$$

where

$$Y_{\nu X} = \frac{1}{2l} D_\nu^m k_\nu^X C_\nu^D(l_X, t), \quad (\nu = H, M) \qquad (26)$$

and l_X is l for X = R and $-l$ for X = L. When the ionic distribution in the solution does not deviate markedly from the thermal equilibrium one, $C_\nu^D(l_X, t)$ in Eq. 26 is reasonably replaced with $C_\nu^{X\infty} \exp(-F\phi_s^X/RT)$. Using Eq. 24, we finally obtain

$$\text{sign}\,(\Phi_H^m) = \text{sign}\left\{C_H^{L\infty}C_M^{R\infty}P_H^L P_M^R - C_H^{R\infty}C_M^{L\infty}P_H^R P_M^L \exp\left[\frac{(\epsilon_{H1} - \epsilon_{M1})(\eta_L - \eta_R)}{k_B T}\right]\right\}, \qquad (27)$$

where we consider only the case of $\epsilon_{\nu 1}^R = \epsilon_{\nu 1}^L$ ($=\epsilon_{\nu 1}$) and $\eta_X = \pm 1$ for simplicity. When both the right and left

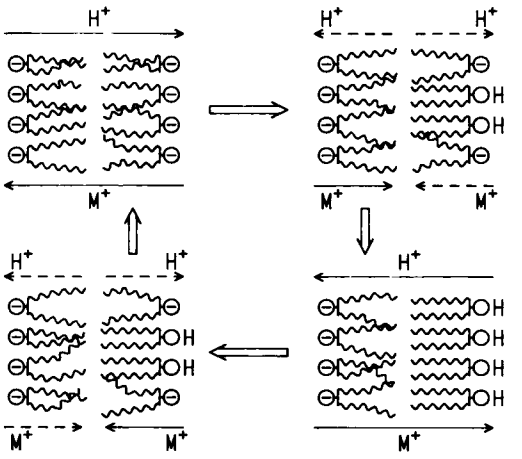

FIGURE 3 Schematic processes for the repetitive phase transitions of the lipid bilayer associated with the cyclic change of the directions of H^+ and M^+ fluxes.

halves of the bilayer are in the liquid crystal state, that is, $\eta_R = \eta_L = -1$, the direction of H^+ flux is given by sign $(C_H^{L\infty} C_M^{R\infty} P_H^L P_M^R - C_H^{R\infty} C_M^{L\infty} P_H^R P_M^L)$, which is positive for the standard case. When the state of the right half is changed to the gel state ($\eta_R = 1$), the direction of H^+ flux is given by sign $(C_H^{L\infty} C_M^{R\infty} P_H^L P_M^R - C_H^{R\infty} C_M^{L\infty} P_H^R P_M^L \times \exp[2(\epsilon_{M1} - \epsilon_{H1})/k_B T])$, which is negative in the standard case ($\epsilon_{M1} > \epsilon_{H1}$). Thus, using Eq. 27, we can estimate whether the reversal of the direction of H^+ flux may be induced by the phase transition.

One of the essential conditions required for the repetitive phase transition in the present system is that the rate of change, $\exp(2\epsilon_{H1}/k_B T)$, in the proton permeability due to the transition is noticeably different from that, $\exp(2\epsilon_{M1}/k_B T)$, for the other cation M^+; the other condition is that the transition has a hysteresis. When these conditions are fulfilled, we can produce the self-sustained oscillation of membrane potential by adjusting the concentrations, $C_H^{X\infty}$ and $C_M^{X\infty}$, of H^+ and M^+ in the left and right side solutions and temperature T.

An approximate expression of the membrane potential ϕ_m is also derived by using Eq. 4, $\Phi_H^m + \Phi_M^m = 0$, and $C_\nu^D(l_X, t) \simeq C_\nu^{X\infty} \exp(-F\phi_s^X/RT)$ as

$$\phi_m = \frac{RT}{F} \ln \left[\frac{C_H^{L\infty} P_H^L \exp(-\epsilon_{H1}\eta_L/k_B T) + C_M^{L\infty} P_M^L \exp(-\epsilon_{M1}\eta_L/k_B T)}{C_H^{R\infty} P_H^R \exp(-\epsilon_{H1}\eta_R/k_B T) + C_M^{R\infty} P_M^R \exp(-\epsilon_{M1}\eta_R/k_B T)} \right]. \quad (28)$$

It is seen from Eq. 28 that ϕ_m becomes minimum for the liquid crystal state ($\eta_R = -1$) and maximum for the gel state ($\eta_R = 1$), as seen in Fig. 2. The amplitude ϕ_{m0} of the potential oscillation is estimated by the difference between the values of ϕ_m for $\eta_R = -1$ and for $\eta_R = 1$ as

$$\phi_{m0} = \frac{RT}{F} \ln \left\{ \frac{C_M^{R\infty} P_M^R \exp[(\epsilon_{M1} - \epsilon_{H1})/k_B T] + C_H^{R\infty} P_H^R}{C_M^{R\infty} P_M^R \exp[(\epsilon_{H1} - \epsilon_{M1})/k_B T] + C_H^{R\infty} P_H^R} \right\} + \frac{2\epsilon_{H1}}{e}. \quad (29)$$

Since the period t_0 of the oscillation coincides with that of the phase transition, t_0 depends on the magnitude of H^+ flux Φ_H^m such that t_0 decreases with increasing Φ_H^m.

Dependence of the potential oscillation on the properties of cations and membranes

We investigate how the wave form of potential oscillation is changed, depending on the properties of cations and membranes, by changing values of the relevant parameters in the model. Values of the cation permeability are considerably different even among alkaline ions: the smaller the radius of hydrated ion, the larger the permeability (36). We show in Fig. 4 the dependences of the oscillation period t_0 on the magnitude of cation permeability P_M ($= P_M^L = P_M^R$) and on the parameter ϵ_{M1} representing the variation of the permeability induced by the phase transition. The oscillation period t_0 decreases with increasing P_M and also with increasing ϵ_{M1}. This comes

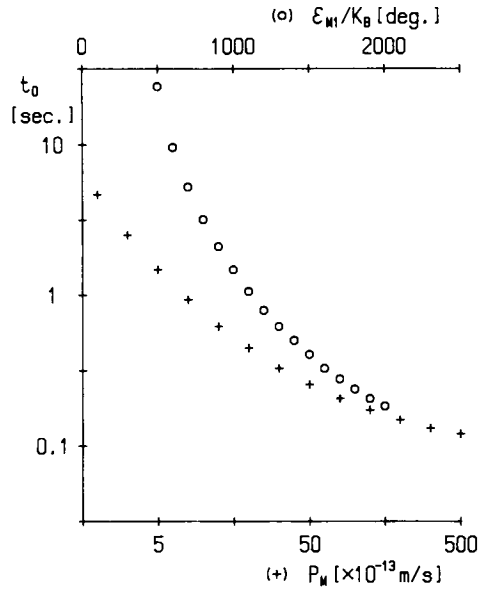

FIGURE 4 The dependences of the period t_0 of potential oscillation on the magnitude of permeability P_M of alkaline ion M and on the parameter ϵ_{M1}, representing the variation of permeability resulting from the phase transition (Eq. 24). Values of the parameters, except for P_M or ϵ_{M1}, are the standard values.

from the facts that the M^+ flux Φ_M^m increases with P_M and also with ϵ_{M1}, as seen from Eqs. 4, 5, and 24, and that the H^+ flux increases with Φ_M^m. The amplitude ϕ_{m0} of the oscillation increases gradually with P_M and ϵ_{M1}, as expected from Eq. 29. The entire permeability includes the other parameter $\epsilon_{\nu 2}^X$, as seen in Eq. 24. However, the oscillation wave form hardly depends on the value of $\epsilon_{\nu 2}^X$, because we assume that the order parameter η_X is changed discontinuously by the phase transition and, as a result, the value of η_X^2 is always near unity.

The dependence of the potential oscillation on the species of lipid molecule comes mainly from the contribution of alkyle chain and polar head. The dependence of the period t_0 on the alkyle chain length N_C is shown in Fig. 5 with the dependence on the H^+ association constant K_H of lipid polar head. Because the temperature T_C of the phase transition changes noticeably with N_C, we must adjust the temperature T of the system for each value of N_C so that the potential oscillation occurs. The optimum temperature at which t_0 is minimized is shown for each case in the figure. The optimum temperature corresponds to the temperature T_C of gel-liquid crystal phase transition, which increases with N_C because of increasing the intermolecular interaction. The reason that t_0 increases with N_C is mainly that the width of the hysteresis $\gamma\Delta w$ increases with N_C. The dependence of t_0 on K_H arises mainly from the fact that the cation concentrations in the solution at the layer surfaces decrease with increasing K_H and then the H^+ flux decreases. The oscillation amplitude ϕ_{m0} hardly depends on N_C and K_H, as seen from Eq. 29.

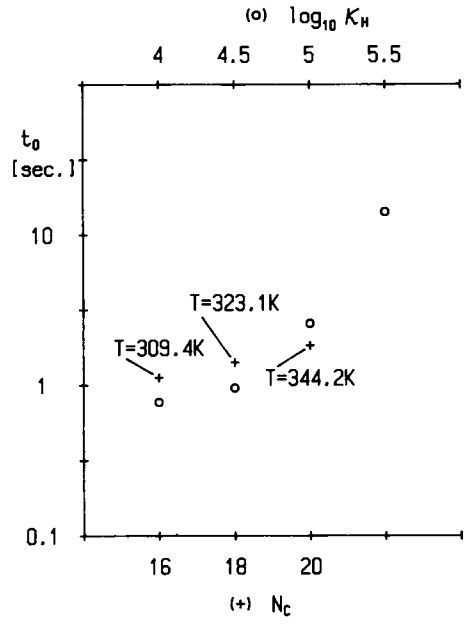

FIGURE 5 The dependences of the oscillation period t_0 on the alkyl chain length N_C of lipid molecule and on the proton association constant K_H of lipid polar head. The figure attached to each cross denotes the value of temperature T used in each calculation (see text).

It has been well known (54) that the composition of lipid molecules is considerably different between the inner and outer halves of the bilayer membrane of many kinds of cells. The dependence of t_0 on the ratio ξ_X of acidic lipid is shown for the two halves of the bilayer in Fig. 6. The period t_0 is rather insensitive to ξ_L, because there is no phase transition in the left half, as seen in Fig. 2. The period t_0 becomes minimal at a definite value of ξ_R. Since the gel state in the right half is more stabilized

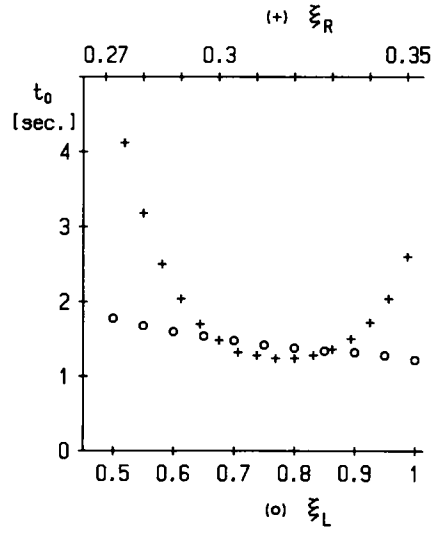

FIGURE 6 The dependences of the oscillation period t_0 on the ratio ξ_X of acidic lipid in the right (X = R) and left (X = L) halves of the bilayer.

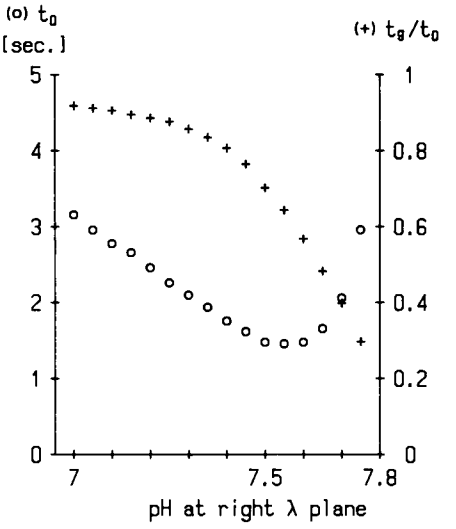

FIGURE 7 The dependences of t_0 and t_g/t_0 on pH in the right-side solution (pH = $-\log C_H^{R\infty}$). t_g is the time interval during which the right half of the bilayer is in the gel state.

with decreasing ξ_R, while the liquid crystal state is done with increasing ξ_R, there exists the optimum value of ξ_R at which the phase transition occurs most easily. The oscillation amplitude ϕ_{m0} hardly depends on ξ_X.

Control of the potential oscillation by the external parameters

We investigate how the potential oscillation is varied by changing temperature T, pH($C_H^{X\infty}$), or the concentration $C_M^{X\infty}$ of M^+ in the bulk solutions. The oscillation may occur in the narrow range of temperature around the phase transition temperature T_C in the thermal equilibrium state. In the standard case, the oscillation takes place for 322.4K < T < 323.5K, where T_C = 323.1K as shown in Fig. 10 (J = 0). The period t_0 of oscillation becomes minimum at T_C.

The dependence of t_0 on pH (= $-\log C_H^{R\infty}$) in the right-side solution is shown in Fig. 7 with that of t_g/t_0 on pH, where t_g is the time interval during which the right half of the bilayer is in the gel state. These dependences arise from the fact that the gel state is more stabilized with decreasing pH, while the liquid crystal state is stabilized with increasing pH. The dependence of t_0 on the concentration $C_M^{X\infty}$ of cation M^+ in the bulk solutions is shown for X = R and L in Fig. 8. The potential oscillation can occur for a finite range of values of the cation concentration. It is seen from Eq. 27 that the reversal of proton flux does not take place for too-high or too-low concentrations. When the difference between $C_M^{R\infty}$ and $C_M^{L\infty}$ is too small, the cations M^+ do not flow across the membrane.

Effect of electric current on the potential oscillation

The dependence of the oscillation period t_0 on the external direct current J is shown in Fig. 9 with that of t_g/t_0.

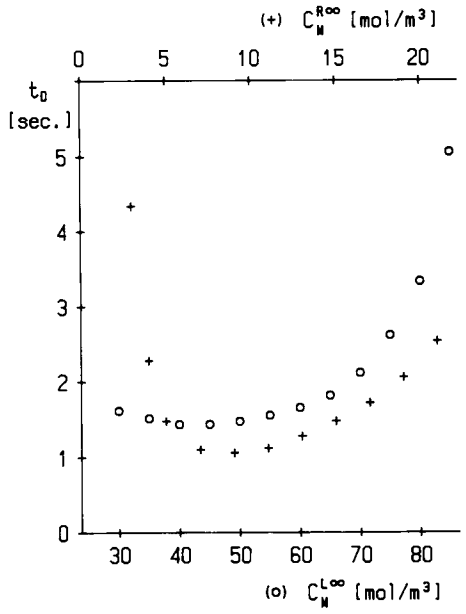

FIGURE 8 The dependences of t_0 on the concentrations, $C_M^{R\infty}$ and $C_M^{L\infty}$, of alkaline ion M^+ in the right- and left-side solutions.

The direction of the current for $J > 0$ is from the left-side solution to the right one, and that for $J < 0$ is reverse. Because the H^+ flux has a tendency to follow the external current J, the H^+ concentration at the surface of the right half of the bilayer increases with J in the case of $J > 0$, while it decreases with increasing $|J|$ in the case of $J < 0$. Therefore, t_0 has a minimum and t_g/t_0 increases with J, as seen in Fig. 9.

The temperature dependence of t_0 is also changed by the external direct current J. We show the effect of J on the temperature dependence in Fig. 10. There appears the different kind of potential oscillation under the application of J in the lower temperature region, as shown

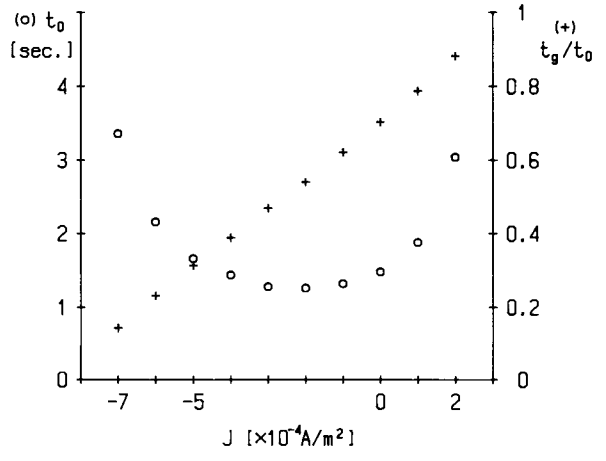

FIGURE 9 The dependences of t_0 and t_g/t_0 on the external current J. The direction of the current is from the left-side solution to the right one for $J > 0$.

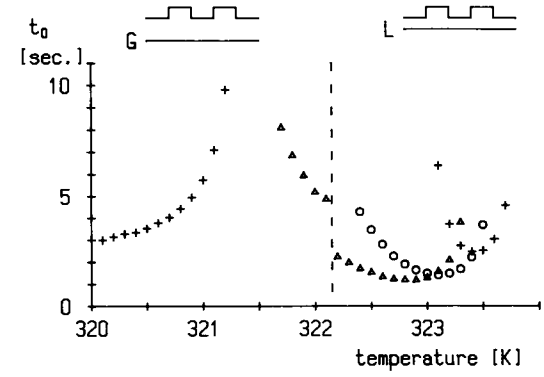

FIGURE 10 The temperature dependence of t_0 in the three cases of $J = 0$ (○), $J = 3 \times 10^{-4}$ A/m² (+), and $J = -3 \times 10^{-4}$ A/m² (△). The state of the left half of the bilayer stays in the liquid crystal one for $T > 322$ K and in the gel one for $T < 322$ K.

in the figure. The oscillation arises from the phase transition of the bilayer, during which the left half of the bilayer stays in the gel state, while it stays in the liquid crystal state in the higher temperature region, which corresponds to the standard case.

Finally, we show the effect of alternating electric current $J(t)$ on the potential oscillation in Fig. 11, where $J(t) = J_0 \sin(2\pi ft)$. The original oscillation for $J_0 = 0$ appears to be modulated only by the external oscillation with a higher frequency. However, it is clearly known by plotting the time intervals τ_n between every successive phase transition that various kinds of oscillation patterns are induced by changing J_0 and/or f. The oscillation patterns obtained include periodic ones with various kinds of periods, quasiperiodic, and chaotic ones. We show also a return map of τ_n for a chaotic oscillation in Fig. 11, where $(\tau_{n+1}/t_0 - 1)$ is plotted against $(\tau_n/t_0 - 1)$ for n = 1, 2, 3, ... Every new point never returns to any old points.

DISCUSSION

The phenomenon of self-sustained potential oscillation has been actively investigated in biomembranes and artificial lipid membranes. It has been found for neural-excitable membranes that the state of self-sustained oscillation of action potentials is induced by reducing the concentration of divalent ion in the external solution (55) or by increasing the pH of the internal solution (56). The mechanism of the oscillation (spontaneous repetitive firing) has been well understood on the basis of the Hodgkin–Huxley equation (55, 57–60). The potential oscillations are due to the functions of voltage-dependent ion channels in the excitable membrane. Therefore, this mechanism is not applicable to the oscillations in the lipid membrane system without protein.

It has been shown that various types of artificial lipid membranes exhibit the self-sustained potential oscillations under suitable conditions. Many workers have

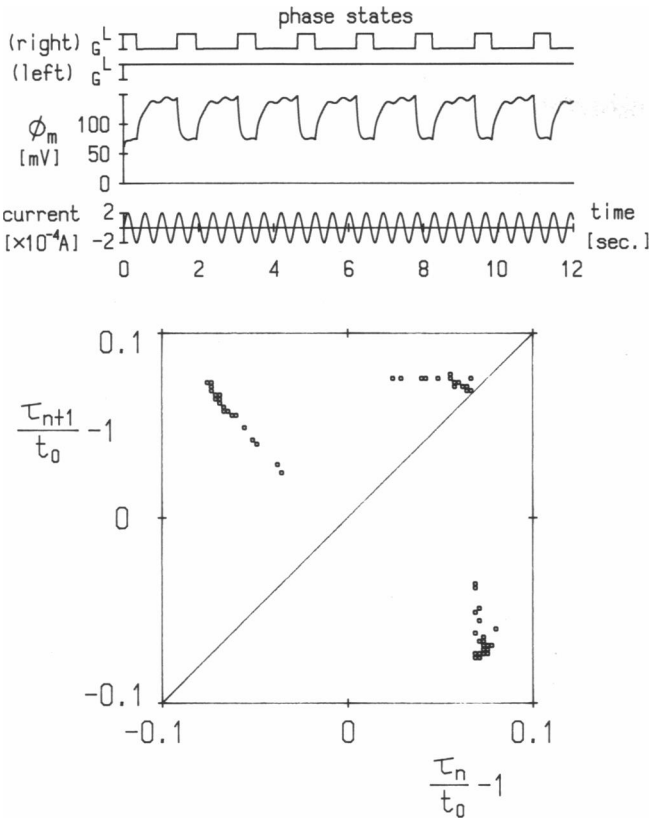

FIGURE 11 The oscillation patterns of the membrane potential ϕ_m and the state of both the right and left halves of the bilayer membrane under the application of a sinusoidal electric current $J_0 \sin(2\pi ft)$, where $J_0 = 0.2$ mA/m^2 and $f = 2.55$ s^{-1}. The return map of the time intervals τ_n between successive phase transitions is also shown, where t_0 is the period in case of $J_0 = 0$.

shown that the self-sustained potential oscillations occur in the system where the fine-pore membrane infiltrated with various kind of lipid molecules is placed between the two solutions, including the different concentrations of a salt or the different kinds of salts (61–65). The two theoretical models have been proposed for the mechanism of the potential oscillations. Toko et al. (64, 66) have presented the model where the self-sustained oscillations are induced by the phase transitions among the three phases of lipid molecules in a pore: oil droplets, spherical micells, and multi-bilayer leaflets. The transitions are driven by the repetitive change of salt concentration in the relevant pore. Because the model is very specialized to treat the fine-pore membrane system, it is hardly applicable to the bilayer membrane system concerned here. Kawakubo (67) has proposed the model that is based on an autocatalytic mechanism for the adsorptive reaction at the gate of each pore. It is not applicable to the present problem either, because no kinds of conformation change have been considered in the model.

Since lipid bilayer membranes are a good model for biological membranes, many workers have studied the oscillations of membrane potentials in the systems composed of lipid bilayers. It is firmly supported by the following observed results that the self-sustained potential oscillations across a lipid bilayer membrane may occur by the mechanism proposed in this paper. Antonov et al. (16) have found that the oscillations of ionic current across the black lipid membrane (single bilayer membrane) may occur under applied voltage only around the temperature of the gel-liquid crystal phase transition of the black lipid membrane. They suggested that the current oscillations were due to the noticeable change in ion permeability during the phase transition. Yoshikawa et al. (18) and Ishii et al. (19) have shown, using the triple bimolecular L-B films of lipid deposited on a porous membrane, that the rhythmic and sustained oscillations of electric potential across the membrane may appear around the phase transition temperature under the suitable gradient of ionic concentrations across the membrane. These oscillations were attributed to the repetitive changes in ion permeabilities induced by the phase transition of the lipid layers. Toko et al. (17) also have shown, using the porous membrane impregnated with polymer multibilayer complexes, that a self-sustained potential oscillation is induced by adjusting the ionic concentrations in the solution regions. They demonstrated clearly, by comparing the thermal properties of the Millipore membrane impregnated with the synthetic bimolecular layers immobilized by polymer with those of simple aqueous dispersions of the immobilized bilayers, that the structure of polymer–bilayer complexes held by the pores was multi-bilayer and that the potential oscillations were associated with the gel-liquid crystal phase transition of the bilayers.

The observed oscillation patterns of electric potential and of ionic current across the bilayer membranes are qualitatively similar to the calculated patterns in the present model. The oscillation patterns may change diversely, depending on the various kinds of quantities, such as the relevant properties of the bilayer membranes, the sort of the ions in the solution regions, the type and magnitude of the ionic concentration gradient, and the number of the bilayers. Therefore, to reproduce reasonably the observed patterns, we need to calculate the oscillation patterns using the parameter values relevant to the observed systems.

Pant and Rosenberg (68) have shown that the sustained, coupled electrical and mechanical oscillations are induced in a lipid bilayer system by adjusting the pHs of the two bathing solutions. It is highly possible that the origin of the mechanical oscillation with the same period as that of the potential oscillation comes from the repetitive phase transition of the membrane. Yoshikawa et al. (69) have shown that the hysteresis loop of the area versus lateral pressure relation for the lipid monolayer on an aqueous solution is characteristically dependent on the chemical stimuli belonging to different taste categories added in the solution. They suggested that the observed

characteristic oscillation patterns induced by various taste compounds added (65, 70) arose from the characteristic dependences of the structural phase transition of lipid molecules upon the compounds. This phenomenon is able to be simulated using our model if we assume the characteristic dependences of phase transition temperature T_C and the width of hysteresis $\gamma\Delta w$ upon the chemical stimuli.

It has been also observed, in some biological and biomimetic membranes, that external electric currents applied across the membrane may induce, modify, or reduce the potential oscillation, depending on their directions and magnitudes (18, 60, 71–75). The calculated results of the current effect correspond reasonably to the observed results. Especially, it has been shown in the excitable biological membranes that the periodic potential oscillations are transformed into quasiperiodic or chaotic oscillations by the sinusoidal current stimulation (76, 77). In this model, the quasiperiodic and chaotic oscillations also appear under the application of sinusoidal current across the membrane. The detailed study of the bifurcation scheme of oscillation period in the present system will be described in a forthcoming paper.

Finally, we consider the effects of the membrane properties, which have not been taken into account in this model, on the membrane potential oscillations. Recently Cruzeiro-Hansson and Mouritsen (78) showed by the computer simulation of the membrane properties based on the 10-state model (27) that the gel-liquid crystal phase transition was accompanied by strong lateral density fluctuations arising from the coexistence of gel and liquid crystal domains. Because in our model we adopted the single domain (molecular field) approximation for the membrane states, the effect of the lateral density fluctuation was not taken into account. However, when the lateral movement of the domain walls is so fast that the walls move over a wide range of the membrane within a period of the potential oscillation, that is, of the repetitive phase transitions, the lateral inhomogeneity of the membrane around the phase transition does not affect the potential oscillation so strongly that this model, based on the lateral homogeneity, becomes unreasonable. If the motion of the domain walls is driven mainly by the lateral diffusion of lipid molecules, it seems to be the case that the motion is quite rapid.

When the domain walls move slowly, that is, when the lateral density fluctuations are long lived, the pattern of oscillation may change noticeably with time. Cruzeiro-Hansson and Mouritsen (78) proposed that the noticeable enhancement of ion permeability at the phase transition (33) came from the relatively high permeation of the ion through the domain walls. Then, the period and stability of the potential oscillation may change with time as the domain walls move, because the apparent permeabilities of ions change with the size of the walls. Antonov et al. (16) suggested that the domain walls worked as a kind of ionic channel. Fuchikami et al. (79) have shown that the simple mathematical model of the chemically excitable membranes leads to autonomous chaotic oscillations of the membrane potential, where the membrane includes two kinds of autocatalytic ion channels distributing homogeneously, and one kind of the channels couples with the other kind of the channels through the membrane potential. Therefore, the interdomain interactions through the potential as well as the lipid–lipid molecular interaction may induce various kinds of oscillations of the membrane potential, and the pattern of the oscillation may change as the domain walls move. The effects of long-lived domains on the potential oscillations are outside of the range of this model and a future problem to be studied.

APPENDIX A

Derivation of Eq. 6 for $C_\nu^D(x, t)$, Eq. 11 for ϕ_s^X, and Eq. 16 for Q_ν^X

We calculate the ion concentrations $C_{\nu 0}(x, t)$ and the electric potential $\phi(x, t)$ in the double-layer region where the ionic distribution is in the thermal equilibrium state. Because the ion flux $\Phi_\nu(x, t)$ vanishes in the equilibrium state, $C_{\nu 0}(x, t)$ is determined by

$$\Phi_\nu(x, t) = -D_\nu^S \frac{\partial C_{\nu 0}(x, t)}{\partial x} - \frac{z_\nu F}{RT} D_\nu^S C_{\nu 0}(x, t) \frac{\partial \phi(x, t)}{\partial x} = 0. \quad \text{(A1)}$$

The potential $\phi(x, t)$ is obtained from the Poisson equation,

$$\epsilon_s \frac{\partial^2 \phi(x, t)}{\partial x^2} = -F \sum_\nu z_\nu C_{\nu 0}(x, t). \quad \text{(A2)}$$

We solve Eqs. A1 and A2 under the following boundary conditions at $x = \lambda_X$ and l_X,

$$C_{\nu 0}(\lambda_X, t) = C_\nu^B(\lambda_X, t), \quad \text{(A3)}$$

$$\left[\frac{\partial \phi(x, t)}{\partial x}\right]_{x=\lambda_X} = 0, \quad \text{(A4)}$$

$$\epsilon_s \left[\frac{\partial \phi(x, t)}{\partial x}\right]_{x=l_X} = \frac{\epsilon_m}{2l} \phi_d - \left(\frac{l_X}{l}\right)\sigma_X. \quad \text{(A5)}$$

The boundary condition (Eq. A4) comes from the assumption that the electric potential is constant in the bulk solution, as mentioned in Appendix B. The condition (Eq. A5) arises from the application of the Gauss law to the membrane surface. We obtain the expressions of $C_{\nu 0}(x, t)$ and $\phi(x, t)$ according to the Gouy–Chapman and Stern theories (22). The concentrations $C_{\nu 0}(x, t)$ of cations and anions are represented as

$$C_{\nu 0}(x, t) = C_\nu^B(\lambda_X, t)\{\coth {}^1/_2[\kappa_X(x - l_X) + a_X]\}^2 \quad \text{for } \nu = \text{M, H} \quad \text{(A6)}$$

$$C_{\nu 0}(x, t) = C_\nu^B(\lambda_X, t)\{\tanh {}^1/_2[\kappa_X(x - l_X) + a_X]\}^2 \quad \text{for } \nu = \text{A, OH}, \quad \text{(A7)}$$

where κ_X and a_X are given by Eqs. 7 and 8, respectively. The surface potential ϕ_s^X, Eq. 11, is obtained by substituting the equation

$$\frac{\partial\phi(x,t)}{\partial x} = -2\left(\frac{\lambda_X}{\lambda}\right)\left(\frac{2RTQ_X}{F\epsilon_s}\right)^{1/2} \times \sinh\left\{\frac{F[\phi(x,t)-\phi(\lambda_X,t)]}{2RT}\right\} \quad (A8)$$

into Eq. A5 and by using the definition $\phi_s^X = \phi(l_X, t) - \phi(\lambda_X, t)$.

The total amount Q_ν^X of ion ν in the X-side double-layer region is obtained by

$$Q_\nu^X(t) = \left(\frac{l_X}{l}\right)\int_{l_X}^{\lambda_X} C_{\nu 0}(x,t)\,dx. \quad (A9)$$

By substituting Eq. A6 or A7 into Eq. A9, we obtain

$$Q_\nu^X(t) = C_\nu^B(\lambda_X,t)\left\{\lambda - l + \frac{2}{\kappa_X}\left[\left(1+\frac{W_X}{Q_X}\right)^{1/2} - 1 + z_\nu\left(\frac{W_X}{Q_X}\right)^{1/2}\right] + \frac{1}{Y_X}\right\}, \quad (A10)$$

$$Y_X = \frac{\kappa_X}{4}\left\{\left[\left(1+\frac{Q_X}{W_X}\right)^{1/2} - \left(\frac{Q_X}{W_X}\right)^{1/2}\right] \times \exp[\kappa_X(\lambda - l)] + 1\right\}. \quad (A11)$$

The value of κ_X is calculated from Eq. 7 for $T = 300$ K and the result is $\kappa_X = 5 \times 10^{13}\sqrt{Q_X/F}\,(1/\mathrm{m})$, where Q_X/F is expressed as moles per cubic meter. Since $(\lambda - l)$ is of the order of 10^{-8} m, Q_X/W_X is $\geq 10^{-5}$, and Q_X/F is >1 in the present calculations, $1/Y_X$ is neglected compared with the other terms. Thus, we obtain Eq. 16 for Q_ν^X.

APPENDIX B

Derivation of Eqs. 12 and 13 for the ion concentration in the bulk solution

To obtain the ion concentrations in the solution regions ($-L < x < -l$ and $l < x < L$ in Fig. 1), we need to consider effects of the ion diffusion from the outside ($x < -L$ and $x > L$) and of the negative charges fixed on the membrane surfaces ($x = -l, l$). The range over which the fixed surface charges affect is quite small ($\lesssim$10 nm) because of the Debye screening. To make the calculation tractable, we divide each solution region into two regions, the bulk solution region ($\lambda \leq |x| \leq L$) and the electric double-layer region ($l \leq |x| \leq \lambda$), as shown in Fig. 1. Because λ is chosen of such a value that it is enough larger than the Debye screening length λ_D, there is no direct effect of the membrane surface charges to the ion distribution in the bulk solution regions.

We consider the ion concentrations $C_\nu^B(x,t)$ in the regions of $\lambda \leq |x| \leq L$. When the external electric current is not extremely large, it can be reasonably assumed that the charge distribution is neutral at any point and any time, that is, $\sum_\nu z_\nu C_\nu^B(x,t) = 0$. Because the electric conductivity in the regions is much higher than that in the membrane, we neglect the voltage gradient due to the external current in the bulk solutions; that is, we assume that the potential $\phi(x)$ is constant over the regions, as shown in Fig. 1. Then, the ion concentrations $C_\nu^B(x,t)$ is determined by the diffusion equation

$$\frac{\partial C_\nu^B(x,t)}{\partial t} = D_\nu^S\frac{\partial^2 C_\nu^B(x,t)}{\partial x^2}. \quad (B1)$$

We solve Eq. B1 under the boundary conditions that $C_\nu^B(x,t)$ takes $C_\nu^{X\infty}$ at $x = L_X$ and $-D_\nu^S\partial C_\nu^B/\partial x$ takes $\Phi_\nu^{X\lambda}(t)$ at $x = \lambda_X$, where $L_X = -L$ for X = L, $L_X = L$ for X = R, and $C_\nu^{X\infty}$ is the fixed ion concentrations at $x = L_X$ and is one of the externally controllable parameters in the present system. It is easily checked by the substitution into Eq. B1 that the solution is given by Eq. 12 for ν = M, A and by Eq. 13 for ν = H, OH. In the above calculations we treat approximately L/λ and L/l as infinity because L, λ, and l are of the order of 10^{-3}, 10^{-8}, and 10^{-9}m, respectively, and we assume that $D_{OH}^S = D_H^S$.

APPENDIX C

Derivation of the coulomb interaction W_{el} represented by Eq. 19

We assume that the ionized lipid molecules are uniformly distributed in the relevant (X) half of the bilayer. Then, the averaged distance (r_0) between the nearest neighboring ionized molecules is evaluated by

$$r_0 = \left[\frac{2}{\pi\xi_X\alpha_X}(A_G\rho_G + A_E\rho_E)\right]^{1/2}, \quad (C1)$$

where α_X is the ionization rate of acidic lipid molecules and given by

$$\alpha_X = [1 + K_H C_H(l_X, t)]^{-1}, \quad (C2)$$

and $\xi_X\alpha_X$ means the ratio of the ionized molecule to all of the lipid molecules in the X side monolayer. We make an approximation of W_{el} with the equation

$$W_{el} = \frac{1}{2}N_I n_{eff}\frac{e^2}{4\pi\epsilon_p}\frac{1}{2r_0}, \quad (C3)$$

where N_I is the number of ionized molecules and given by $(N\xi_X\alpha_X/2)$, n_{eff} is the number of ionized molecules interacting effectively with one ionized molecule, and ϵ_p is the dielectric constant of the polar head region. The strength w of coulomb interaction defined in Eq. 19 is represented as

$$w = \omega(\xi_X\alpha_X)^{3/2} = \frac{e^2 n_{eff}}{32\sqrt{2\pi A_G}\epsilon_p}(\xi_X\alpha_X)^{3/2}. \quad (C4)$$

The value of ω is estimated by using $\epsilon_p = 20\epsilon_0$, $n_{eff} = 6$, $e = 1.6 \times 10^{-19}$ C, and $A_G = 20.4 \times 10^{-16}$ cm^2, and the result is $1.7 \times 10^3 k_B$. Therefore, we choose the value of ω in the range of $5 \times 10^2 k_B$–$5 \times 10^3 k_B$, as shown in Table 1.

Received for publication 24 July 1992 and in final form 8 January 1993.

REFERENCES

1. Kobatake, Y., I. Tasaki, and A. Watanabe. 1971. Phase transition in membrane with reference to nerve excitation. *Adv. Biophys.* 2:1–31.
2. Ueda, I., I. Inoue, and Y. Kobatake. 1973. Studies of excitable membrane formed on the surface of protoplasmic drops isolated from *Nitella*. II. Tension at the surface of protoplasmic drops. *Biochim. Biophys. Acta.* 318:326–334.
3. Inoue, I., N. Ishida, and Y. Kobatake. 1973. Studies of excitable membrane formed on the surface of protoplasmic drops isolated from *Nitella*. IV. Excitability of the drop membrane in various compositions of the external salt solutions. *Biochim. Biophys. Acta.* 330:27–38.
4. Inoue, I., Y. Kobatake, and I. Tasaki. 1973. Excitability instability and phase transitions in squid axon membrane under internal perfusion with dilute salt solutions. *Biochim. Biophys. Acta.* 307:471–477.
5. Lelkes, P. I. 1979. Potential dependent rigidity changes in lipid membrane vesicles. *Biochem. Biophys. Res. Commun.* 90:656–662.

6. Tasaki, I. 1982. Physiology and Electrochemistry of Nerve Fibers. Academic Press, New York. 348 pp.
7. Papakostidis, G., G. Zundel, and E. Mehl. 1972. Na^+-K^+-dependent conformation change of proteins of excitable membranes. *Biochim. Biophys. Acta.* 288:277–281.
8. Boonstra, J., S. Nelemans, A. Feijen, A. Bierman, E. J. J. Van Zoelen, P. T. Van der Saag, and S. W. Delaat. 1982. The effect of fatty acids on plasma membrane lipid dynamics and cation permeability in neuroblastoma cells. *Biochim. Biophys. Acta.* 692:321–329.
9. Georgescauld, D., and H. Duclohier. 1978. Transient fluorescence signals from pyrene labeled pike nerves during action potential: possible implications for membrane fluidity changes. *Biochem. Biophys. Res. Commun.* 85:1186–1191.
10. Corda, D., C. Pasernak, and M. Shinitzky. 1982. Increase in lipid microviscosity of unilamellar vesicles upon the creation of transmembrane potential. *J. Membr. Biol.* 65:235–242.
11. Linden, C. D., and C. F. Fox. 1975. Membrane physical state and function. *Accounts Chem. Res.* 8:321–327.
12. Vaz, W. C., E. C. C. Melo, and T. E. Thompson. 1989. Translational diffusion and fluid domain connectivity in a two-component, two phase phospholipid bilayer. *Biophys. J.* 56:869–876.
13. Träuble, H., and H. Eibl. 1974. Electrostatic effects on lipid phase transitions: membrane structure and ionic environment. *Proc. Natl. Acad. Sci. USA.* 71:214–219.
14. Blatt, F. J. 1974. Temperature dependence of the action potential in *Nitella flexilis. Biochim. Biophys. Acta.* 339:382–389.
15. DeSimone, J. A., and G. L. Heck. 1980. An analysis of the effects of stimulus transport and membrane charge on the salt, acid and water-response of mammals. *Chem. Senses.* 5:295–316.
16. Antonov, V. F., V. V. Petrov, A. A. Molnar, D. A. Predvoditelev, and A. S. Ivanov. 1980. The appearance of single-ion channels in unmodified lipid bilayer membranes at the phase transition temperature. *Nature (Lond.).* 283:585–586.
17. Toko, K., N. Nagashima, S. Iiyama, K. Yamafuji, and T. Kunitake. 1986. Self-oscillation of electric potential of a porous membrane impregnated with polymer multibilayer complexes. *Chem. Lett.* 1986:1375–1378.
18. Yoshikawa, K., T. Omachi, T. Ishii, Y. Kuroda, and K. Iiyama. 1985. Unique electronic property of a Langmuir–Blodgett film of dioleyl lecithin deposited on a porous membrane. *Biochem. Biophys. Res. Commun.* 133:740–744.
19. Ishii, T., Y. Kuroda, T. Omochi, and K. Yoshikawa. 1986. Spontaneous pulsing in a porous membrane covered with a Langmuir–Blodgett film of dioleoyllecithin separating equimolar NaCl and KCl aqueous solutions. *Langmuir.* 2:319–321.
20. Smith, R. L., and E. Oldfield. 1984. Dynamical structure of membranes by deutrium NMR. *Science (Wash. DC).* 225:280–288.
21. Naito, M., N. Fuchikami, N. Sasaki, and T. Kambara. 1991. Model for the dynamic responses of taste receptor cells to salty stimuli. I. Function of lipid bilayer membranes. *Biophys. J.* 59:1218–1234.
22. Lakshminarayanaiah, N. 1984. Equations of Membrane Biophysics. Academic Press, New York. 426 pp.
23. DeSimone, J. A., G. L. Heck, and S. K. DeSimone. 1986. An empirical relation for the surface potential of phosphatidic acid monolayers: its dependence on calcium and the role of double layer theory. *In* Electrical Double Layers in Biology. M. Blank, editor. Plenum Press, New York. 17–29.
24. MacDonald, R. C., S. A. Simon, and E. Baer. 1976. Ionic influences on the phase transition of dipalmitoylphosphatidylserine. *Biochemistry.* 15:885–891.
25. Watts, A., K. Harlos, W. Maschke, and D. Marsh. 1978. Control of the structure and fluidity of phosphatidylglycerol bilayers by pH titration. *Biochim. Biophys. Acta.* 510:63–74.
26. Caille, A., A. Rapini, M. J. Zuckermann, and A. Cros. 1978. A simple model for phase transitions in monolayers and bilayers of lipid molecules. *Can. J. Phys.* 56:348–357.
27. Caille, A., D. Pink, F. de Verteuil, and M. J. Zuckermann. 1980. Theoretical models for quasi-two dimensional mesomorphic menolayers and membrane bilayers. *Can. J. Phys.* 58:581–611.
28. Mouritsen, O. G., A. Boothroyd, R. Harris, N. Jan, T. Lookman, L. MacDonald, D. A. Pink, and M. J. Zuckermann. 1983. Computer simulation of the main gel–liquid crystal transition of lipid bilayers. *J. Chem. Phys.* 79:2027–2041.
29. Nagle, J. F. 1980. Theory of the main lipid bilayer phase transition. *Annu. Rev. Phys. Chem.* 31:157–195.
30. Kambara, T., and N. Sasaki. 1984. A self-consistent chain model for the phase transition in lipid bilayer membranes. *Biophys. J.* 46:371–382.
31. Sillerud, L. O., and R. E. Barnett. 1982. Lack of transbilayer coupling in phase transitions of phosphatidylcholine vesicles. *Biochemistry.* 21:1756–1760.
32. Overath, P., and H. Träuble. 1973. Phase transitions in cells, membranes, and lipids of *Escherichia coli.* Detection by fluorescent probes, light scattering, and dilatometry. *Biochemistry.* 12:2625–2634.
33. Papahadjopoulos, D., K. Jacobson, S. Nir, and T. Isac. 1973. Phase transitions in phospholipid vesicles. Fluorescence polarization and permeability measurements concerning the effect of temperature and cholesterole. *Biochim. Biophys. Acta.* 311: 330–348.
34. Doniach, S. 1978. Thermodynamic fluctuations in phospholipid bilayers. *J. Chem. Phys.* 68:4912–4916.
35. Nagle, J. F., and H. L. Scott, Jr. 1978. Lateral compressibility of lipid mono- and bilayers. Theory of membrane permeability. *Biochim. Biophys. Acta.* 513:236–243.
36. Georgallas, A., J. D. MacArthur, X.-P. Ma, C. V. Nguyen, and G. R. Palmer. 1987. The diffusion of small ions through phospholipid bilayers. *J. Chem. Phys.* 86:7218–7226.
37. Johnson, S. M., and A. D. Bangham. 1969. Potassium permeability of single compartment liposomes with and without valinomycin. *Biochim. Biophys. Acta.* 193:82–91.
38. Papahadjopoulos, D., S. Nir, and S. Ohki. 1971. Permeability properties of phospholipid membranes: effects of cholesterol and temperature. *Biochim. Biophys. Acta.* 266:561–583.
39. Hauser, H., D. Oldani, and M. C. Phillips. 1973. Mechanism of ion escape from phosphatidylcholine and phosphatidylserine single bilayer vesicles. *Biochemistry.* 12:4507–4517.
40. Nichols, J. W., and D. W. Deamer. 1980. Net proton–hydroxyl permeability of large unilamellar liposomes measured by an acid–base titration technique. *Proc. Natl. Acad. Sci. USA.* 77:2038–2042.
41. Pike, M. M., S. R. Simon, J. A. Balschi, and C. S. Springer, Jr. 1982. High-resolution NMR studies of transmembrane cation transport: use of an aqueous shift reagent for ^{23}Na. *Proc. Natl. Acad. Sci. USA.* 79:810–814.
42. El-Mashak, E. M., and T. Y. Tsong. 1985. Ion selectivity of temperature-induced and electric field induced pores in dipalmitoylphosphatidylcholine vesicles. *Biochemistry.* 24:2884–2888.
43. Kell, D. S., and J. G. Morris. 1980. Formulation and some biological uses of a buffer mixture where buffering capacity is relatively independent of pH in the range pH 4–9. *J. Biochem. Biophys. Methods.* 3:143–150.
44. Nozaki, Y., and C. Tanford. 1981. Proton and hydroxide ion per-

meability of phospholipid vesicles. *Proc. Natl. Acad. Sci. USA.* 78:4324–4328.

45. Deamer, D. W., and J. W. Nichols. 1983. Proton-hydroxide permeability of liposomes. *Proc. Natl. Acad. Sci. USA.* 80:165–168.
46. Cafiso, D. S., and W. L. Hubbell. 1983. Electrogenic H^+/OH^- movement across phospholipid vesicles measured by spin-labeled hydrophobic ions. *Biophys. J.* 44:49–57.
47. Krishnamoorthy, G., and P. C. Hinkle. 1984. Non-ohmic proton conductance of mitochondria and liposomes. *Biochemistry.* 23:1640–1645.
48. Grzesiek, S., and N. A. Dencher. 1986. Dependence of ΔpH-relaxation across vesicular membranes on the buffering power of bulk solutions and lipids. *Biophys. J.* 50:265–276.
49. Ohki, S., and R. Kurland. 1981. Surface potential of phosphatidylserine monolayers II. Divalent and monovalent ion binding. *Biochim. Biophys. Acta.* 645:170–176.
50. Tsui, F. C., D. M. Ojcius, and W. L. Hubbell. 1986. The intrinsic pK_a values for phosphatidylserine and phosphatidylethanolamine in phosphatidylcholine host bilayers. *Biophys. J.* 49:459–468.
51. Ohki, S. 1985. The origin of electrical potential in biological systems. *In* Comprehensive Treatise of Electrochemistry. Vol. 10. Biochemistry. S. Srinivasan, Y. A. Chizmadzhev, J. O'M. Bockris, B. E. Conway, and E. Yeager, editors. Plenum Press, New York. 1–130.
52. Mitaku, S., and T. Date. 1982. Anomalies of nanosecond ultrasonic relaxation in the lipid bilayer transition. *Biochim. Biophys. Acta.* 688:411–421.
53. Earnshaw, J. C., and G. E. Crawford. 1989. Viscoelestic relaxation of bilayer lipid membranes. II. Temperature dependence of relaxation time. *Biophys. J.* 55:1017–1021.
54. Houslay, M. D., and K. K. Stanley. 1982. Dynamics of Biological Membranes. John Wiley & Sons, New York. 330 pp.
55. Huxley, A. R. 1959. Ion movements during nerve activity. *Ann. NY Acad. Sci.* 81:221–246.
56. Tasaki, I., I. Shinger, and T. Takenaka. 1965. Effects of internal and external ionic environment on excitability of squid giant axon. A macromolecular approach. *J. Gen. Physiol.* 48:1095–1123.
57. Frankenhauser, B., and A. L. Hodgkin. 1957. The action of calcium on the electrical properties of squid axons. *J. Physiol. (Lond.).* 137:218–244.
58. Guttman, R., and R. Barnhill. 1970. Oscillation and repetitive firing in squid axones. Comparison of experiments with computations. *J. Gen. Physiol.* 55:104–118.
59. Rinzel, J., and R. N. Miller. 1980. Numerical calculation of stable and unstable periodic solutions to the Hodgkin–Huxley equations. *Math. Biosci.* 49:27–59.
60. Matsumoto, G., K. Kim, T. Uehara, and J. Shinada. 1980. Electrical and computer simulations upon the nervous activities of squid giant axons at and around the state of spontaneous repetitive firing of action potentials. *J. Phys. Soc. Jpn.* 49:906–914.
61. Yoshida, M., N. Kamo, and Y. Kobatake. 1972. Transport phenomena in a model membrane accompanying a conformational change: membrane potential and ion permeability. *J. Membr. Biol.* 8:389–402.
62. Von Klitzing, L., M. Daber, and H. D. Bergeder. 1973. Über das auftreten autonomer spannungsimpulse (spikes) an lipoid/elektrolyt-grenzflächen. *Biophysik.* 9:166–171.
63. Arisawa, J., and T. Furukawa. 1977. Sustained oscillations of membrane potential in a DOPH model membrane in a constant applied pressure gradient. *J. Membr. Sci.* 2:303–307.
64. Toko, K., J. Nitta, and K. Yamafuji. 1981. Dynamic aspect of a phase transition in DOPH–Millipore membranes. *J. Phys. Soc. Jpn.* 50:1343–1350.
65. Yoshikawa, K., K. Sakabe, Y. Matsubara, and T. Ota. 1984. Oscillation of electrical potential in a porous membrane doped with glycerol α-monooleate induced by an Na^+/K^+ concentration gradient. *Biophys. Chem.* 20:107–109.
66. Toko, K., M. Tsukiji, S. Iiyama, and K. Yamafuji. 1986. Self-sustained oscillations of electric potential in a model membrane. *Biophys. Chem.* 23:201–210.
67. Kawakubo, T. 1986. Critical change of ion conductance and self-sustained potential oscillation in artificial membrane systems. *Biophys. Chem.* 23:229–235.
68. Pant, H. C., and B. Rosenberg. 1971. Sustained, coupled electrical and mechanical oscillations in a biomolecular lipid membrane in the presence of inorganic ions. *Biochim. Biophys. Acta.* 225:379–381.
69. Yoshikawa, K., M. Shoji, and T. Ishii. 1989. Characteristic effects of taste-compounds on the dynamic behavior of oleate-monolayer. *Biochem. Biophys. Res. Commun.* 160:699–704.
70. Yoshikawa, K., K. Sakabe, Y. Matsubara, and T. Ota. 1985. Self-excitation in a porous membrane doped with sorbitan monooleate (SPAN-80) induced by an Na^+/K^+ concentration gradient. *Biophys. Chem.* 21:33–39.
71. Kamo, N., T. Yoshioka, Yoshida, and T. Sugita. 1973. Transport phenomena in a model membrane accompanying a conformational change: transient processes in response to external stimuli. *J. Membr. Biol.* 12:193–205.
72. Kobatake, Y. 1975. Physicochemical problems in excitable membranes. *Adv. Chem. Phys.* 29:319–336.
73. Mueller, P. 1980. Action potentials in lipid bilayers. *Ber. Bunsenges. Phys. Chem.* 84:341–347.
74. Monnier, A. M. 1982. Histoire et interet de l'etude des membranes artificielles electriquement excitables. *Rev. Can. Biol. Exp.* 41:47–63.
75. Toko, K., M. Tsukiji, S. Ezaki, and K. Yamafuji. 1984. Current–voltage characteristics and self-sustained oscillations in dioleyl phosphate–Millipore membranes. *Biophys. Chem.* 20:39–59.
76. Hayashi, H., M. Nakano, and K. Hirakawa. 1982. Chaos in the self-sustained oscillation of an excitable biological membrane under sinusoidal stimulation. *Phys. Lett.* 88A:265–266.
77. Matsumoto, G., K. Aihara, M. Ichikawa, and A. Tasaki. 1984. Periodic and nonperiodic responses of membrane potentials in squid giant axons during sinusoidal current stimulation. *J. Theor. Neurobiol.* 3:1–14.
78. Cruzeiro-Hansson, L., and O. G. Mouritsen. 1988. Passive ion permeability of lipid membranes modelled via lipid–domain interfacial area. *Biochim. Biophys. Acta.* 944:63–72.
79. Fuchikami, N., N. Sawashima, M. Naito, and T. Kambara. 1993. Model of chemically excitable membranes generating autonomous chaotic oscillations. *Biophys. Chem.* In press.